Fabrication of mid-infrared frequency-selective surfaces by soft lithography

Kateri E. Paul, Cheng Zhu, J. Christopher Love, and George M. Whitesides

We describe the fabrication of large areas (4 cm^2) of metallic structures or aperture elements that have ~100–350-nm linewidths and act as frequency-selective surfaces. These structures are fabricated with a type of soft lithography—near-field contact-mode photolithography—that uses a thin elastomeric mask having topography on its surface and is in conformal contact with a layer of photoresist. The mask acts as an optical element to create minima in the intensity of light delivered to the photoresist. Depending on the type of photoresist used, lines of, or trenches in, photoresist are formed on the substrate by exposure, development, and lift-off. These surfaces act as bandpass or bandgap filters in the infrared.

OCIS codes: 260.3060, 350.2450, 220.4000, 220.3740.

1. Introduction

In this paper we describe the application of a soft lithographic technique—near-field contact-mode photolithography—to the fabrication of frequency-selective surfaces (FSS). We fabricated an array of circular loops having critical dimensions as small as 100 nm in a thin layer of aluminum over areas greater than 4 cm^2. These loops act as filters in the range of 3–13 μm, depending on the diameters of the loops. Soft lithography has the ability to fabricate large areas of FSS for the infrared quickly and inexpensively.

The utility of FSS in the microwave region has been known since the 1960s for controlling electromagnetic transmission and reception. From the microwave region to the far-infrared region, technologies including machining and traditional photolithography are well established for the fabrication of FSS.[1,2] Below that range, when the wavelength of interest is in the mid-infrared and infrared regions (0.8–20 μm) or the visible region (0.8–0.4 μm), the feature sizes necessary for FSS are smaller than those that traditional photolithography can easily generate. More complex techniques—extreme-ultraviolet lithography, x-ray lithography, and e-beam writing—have been used to fabricate features in this range and specifically to fabricate FSS.[3–6] Although these techniques work well to generate test structures, they are complex, expensive, inapplicable to nonplanar surfaces, and inappropriate for certain materials. Soft lithography[7,8]—a collection of techniques that includes printing, molding, and certain types of phase-shift photolithography and that shares use of an elastomeric organic polymer element for pattern transfer—provides a new route to these types of structures. Soft lithographic techniques are intrinsically simple and inexpensive; they can be applied to fabrication on curved surfaces and they accept a wide range of materials. They do not have the global dimensional stability of high-resolution photolithography and are thus better suited for the single-level fabrication of the type required for FSS and related optical structures than for multilevel fabrication of the type required for complex microelectronic systems.

Among those soft lithographic techniques able to generate features smaller than 100 nm are near-field contact-mode lithography,[9,10] topographically directed photolithography,[11] topographically directed etching,[12,13] and controlled overetching.[14] As a demonstration of the utility of soft lithography to generate optical structures in the infrared region of the spectrum, we use near-field contact-mode lithography to fabricate mid-infrared FSS consisting of patterned aluminum films on single-crystal calcium fluoride windows or optical-grade silicon wafers.

The authors are with the Department of Chemistry and Chemical Biology, Harvard University, 12 Oxford Street, Cambridge, Massachusetts 02138-2902. The e-mail address for G. M. Whitesides is gwhitesides@gmwgroup.harvard.edu.

Received 2 January 2001; revised manuscript received 12 June 2001.

0003-6935/01/254557-05$15.00/0

We obtained arrays of frequency-selective elements consisting of circular loops with diameters of 0.85–2.15 μm. Each element has a linewidth between 100 and 350 nm, depending on the photoresist used, and the fabrication technique generates a dense array over areas of 1–4 cm^2. Optical measurement shows that the patterned surface consisting of trenches in an aluminum film acts as a bandpass filter, whereas aluminum rings act as a bandgap filter.

2. Experiment

The mechanism for near-field contact-mode lithography has been described in detail previously.[9,10,15,16] We first make a phase mask by casting poly(dimethylsiloxane) (PDMS) precursor (Sylgard 184, Dow Corning, Midland, Mich.) on masters having the desired features. To prevent sagging of the mask—that is, to make the mask stiffer—we used a high ratio of curing agent to precursor, 1:6, as compared with the ratio of 1:10 recommended by the manufacturer. Although recent research shows that the modulus of the cured polymer is at its highest at the recommended mixture,[17] in our experience stamps with a higher ratio of the cross-linker cast against 400-nm tall features do not sag into contact across the surface of the mask. We brought the stamp into conformal contact with a substrate coated with a thin layer (~200 nm) of photoresist. For the fabrication of bandpass filters, we used a positive resist (Shipley 1805, Microchem Corp., Newton, Mass.) on CaF_2 windows (Harrick Scientific, Ossining, N.Y., and Janos Technology, Townshend, Ver.). CaF_2 is slightly soluble in water and transmits light in the wavelength range from 1.5 to 9 μm. An image-reversal photoresist (AZ 5206, Clariant, Somerville, N.J.) was used on optical-grade silicon wafers (Valley Design, Westford, Mass.) to fabricate the bandgap filters. We exposed the photoresist surface to broadband UV light (365–436 nm, Karl Süss Mask Aligner, MJB300) through the elastomeric phase mask, typically for ~2 s. Positive photoresist, after it was developed, resulted in photoresist features corresponding to the edge of the features on the mask on the CaF_2 substrate, whereas the image-reversal resist resulted in a trench in the photoresist surface. Finally, we evaporated 50 nm of aluminum onto the sample and lifted off the photoresist and metal using acetone. Fig. 1 shows a schematic of the procedure.

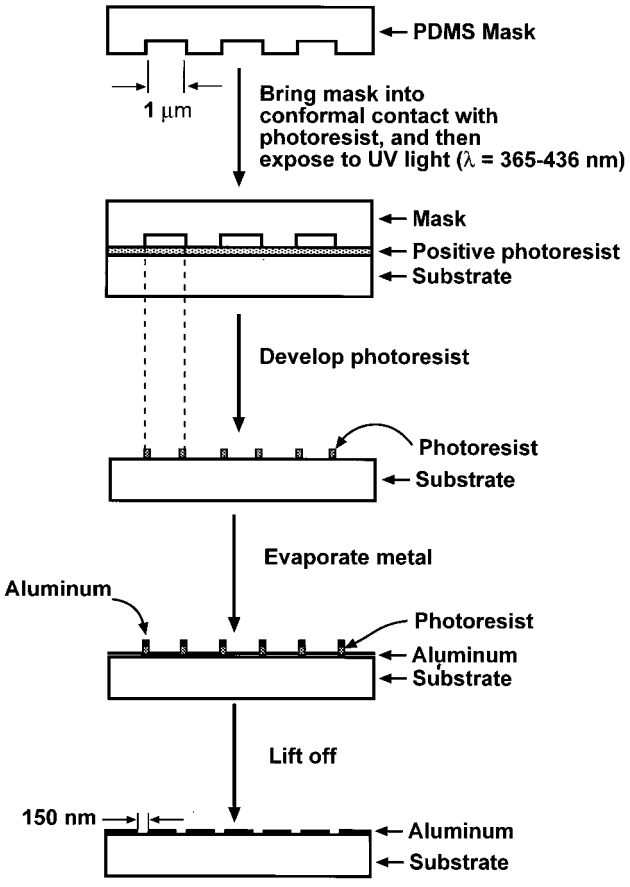

Fig. 1. Schematic illustration of the procedure for fabricating mid-infrared FSS by near-field contact-mode photolithography.

3. Results and Discussion

A. Fabrication of Frequency-Selective Surfaces by Near-Field Contact-Mode Photolithography

We obtained arrays of rings having diameters of 850 nm (Fig. 2) and 1.85 μm (Fig. 3) over large areas. The diameter of the ring obtained is smaller than that of the original recessed well on the mask because the features in phase-shift lithography arise on the inside of the area that is recessed, which is due to a combination of sagging and loss of transmitted light at the PDMS–air interface.[16] In Fig. 2, we used a mask having roughly circular wells in PDMS with average diameters of 950 nm; use of this mask in phase-shift photolithography gives rise to rings of photoresist with diameters of ~850 nm. For the features shown in Fig. 3, the mask consisted of recessed wells in PDMS having diameters of ~2.15 μm. The mask generates rings of photoresist with diameters of ~1.85 μm.

We used an image-reversal photoresist to fabricate arrays of trenches in the layer of photoresist with outer diameters of ~2.15 μm and inner diameters of ~1.45 μm using a PDMS mask having recessed wells with diameters of 2.15 μm (Fig. 4). The diffusion that occurs in the exposed photoresist during the postexposure bake increases the linewidth of the trench in the photoresist, and therefore the resulting rings after deposition of aluminum and lift-off are ~350 nm wide. In all cases, we characterized the features visually by scanning electron microscopy (LEO 982, Leo Electron Microscopy Inc., Thornwood, N.Y.).

B. Optical Measurement

We used a Nicolet Fourier-transform infrared spectrometer in transmission mode to optically characterize the samples. A clean substrate served as a sample for the background spectrum that was then

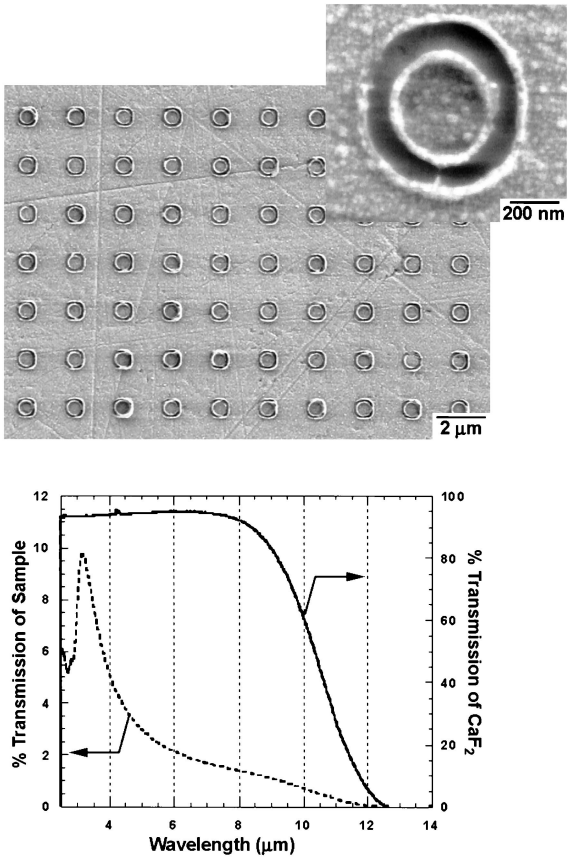

Fig. 2. Top, scanning electron micrographs of rings with a diameter of ~850 nm. The light regions are aluminum and the dark regions are CaF_2. These features occur uniformly over the 1-in.-(2.54-cm-) diameter window. The width of the trench in the aluminum is approximately 100 nm. Bottom, infrared transmission curve obtained for the array shown above. The solid curve shows the spectrum of the CaF_2 background and the dotted curve shows the average curve for the sample with a transmission peak at 3.18 μm.

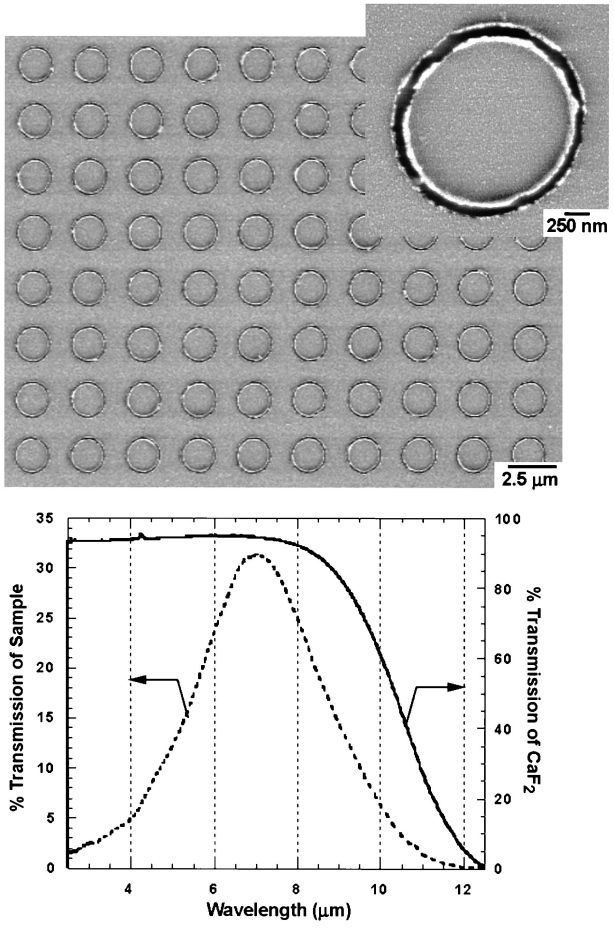

Fig. 3. Top, scanning electron micrographs of rings with a diameter of 1.85 μm. The light areas of the surface are aluminum and the dark areas are calcium fluoride. Bottom, infrared transmission curve for the FSS. The solid curve shows the transmission of the CaF_2 background and the dotted curve shows the average transmission curve for the sample with a peak at 7.07 μm.

subtracted automatically from the sample spectrum. The sample curves (dotted curves) shown in Figs. 2, 3, and 4 are averages of data obtained from at least four regions of the surface of the sample. Spectra obtained from different regions were similar, exhibiting small variations in peak intensity, probably because of incomplete lift-off. The width of the feature and the spacing of the aperture elements determine the shape of the resonance peak and are related by a quality factor Q. The width of the trench formed by lift-off of the metal layer in both cases of positive photoresist is approximately 100 nm; thus the ratio of feature size to linewidth is around 10, and the arrays give good optical performance. Peaks or bands with a smaller full width at half-maximum (FWHM) could be obtained with narrower linewidths and peaks, or bands with higher intensity could be obtained with more densely packed arrays of elements.

The theoretical value for the resonance wavelength of a circular loop is given by

$$\lambda_r \sim n_{\text{eff}} \pi D. \tag{1}$$

Here λ_r is the resonance wavelength, D is the diameter of the circular loop, and n_{eff} is the effective index of refraction of the medium surrounding the array.[2] The value of n_{eff} is determined by

$$n_{\text{eff}} = [(\varepsilon_1 + \varepsilon_2)/2]^{1/2}. \tag{2}$$

Here ε_1 and ε_2 are the permittivity of the substrate (either silicon or calcium fluoride) and the medium (air).[4] The bandpass samples shown in Fig. 2 show transmission at 3.18 μm; this value compares well with a predicted value of 3.25 μm for loops having diameters of 850 nm. Features shown in Fig. 3 also compare well with theoretical values with a predicted value of 7.07 μm for a resonant peak with 1.85-μm loops. The sample in Fig. 4 has the greatest difference between theoretical and experimental results. Loops of aluminum having diameters of 2.15 μm on silicon should have a resonant wavelength at 16.9 μm, where a stop in transmission at 12.9 μm was measured. One possible explanation for this difference could be the presence of the native oxide on the surface of the silicon substrate. Using ellipsometry,

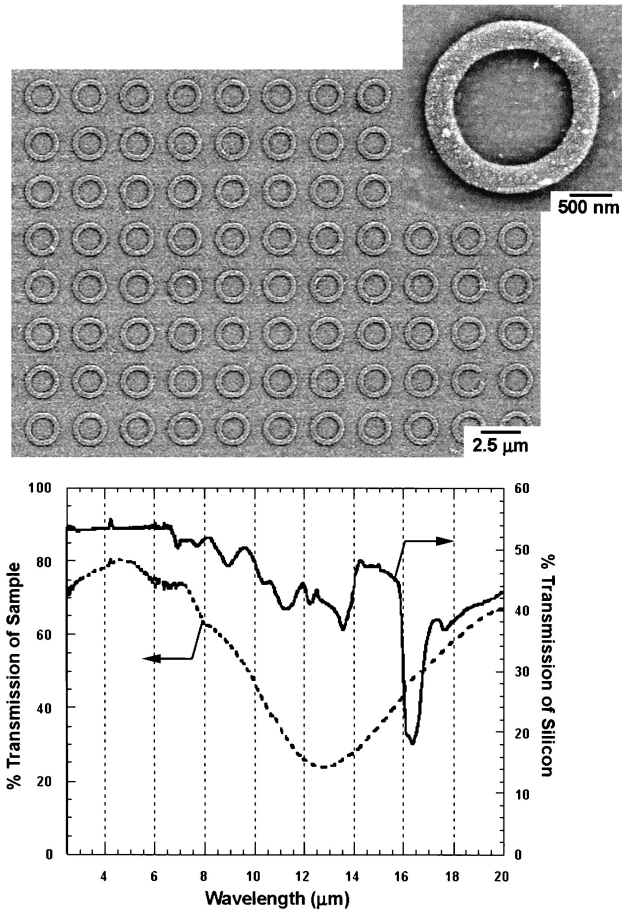

Fig. 4. Top, scanning electron micrograph of a bandgap filter of aluminum rings fabricated on optical-grade silicon. The rings have a diameter of 2.15 μm and a linewidth of ~350 nm. Bottom, the solid curve shows the transmission of the silicon background and the dotted curve shows the average transmission curve for the FSS shown above. The transmission band occurs at 12.9 μm.

we measured the thickness of the oxide layer to be 10 nm. Because the evanescent wave generated in the aluminum ring would first have to pass through the oxide layer before reaching the silicon substrate, the n_{eff} of the silicon–air media could be reduced from 2.50 to 1.91, which is the calculated effective index necessary to generate a band stop at 12.9 μm with loops of 2.15 μm.

4. Conclusions

Near-field contact-mode photolithography provides a simple and low-cost route to fabricate large arrays of elements that act as a frequency-selective surface in the mid-infrared. Photoresist masters generated by conventional photolithography are used to produce elastomeric phase masks, which then transfer the outline of the pattern on the mask to form an array of rings or trenches in a layer of photoresist. Deposition of a metal film—in this case, aluminum—followed by lift-off forms the FSS.

The advantages of this technique for fabricating single-layer optical devices are (i) the original pattern on the elastomeric mask is defined by any of a number of conventional or soft lithography techniques; (ii) a single exposure generates an array of features in parallel across a large area (>4 cm^2); and (iii) the technique can be used on curved or spherical substrates and, in principle, can be used in low-cost replication methods such as rotary printing.[18] Near-field phase-shifting photolithography is well suited for single-level fabrication of the kind required here. In comparison with other lithographic tools, for example, e-beam and ion-beam lithography—the key disadvantage of this technique is that completely arbitrary patterns (especially nonclosed patterns) are difficult to generate because the *edges* of the pattern on the mask become the pattern in the photoresist; this generally limits the technique to closed figures. A crossed dipole, for example, would be impossible to fabricate in one step with near-field contact-mode lithography by use of an elastomeric stamp. As new techniques are added to the set of soft lithography, the ability to generate features for FSS beyond closed loops may become possible.

This research was supported in part by the National Science Foundation (NSF) (PHY-9312572) and in part by the U.S. Office of Naval Research and the Defense Advanced Research Projects Agency. We also used the Materials Research Science and Engineering Center Shared Facilities supported by the NSF under award DMR-9400396. J. C. Love gratefully acknowledges the U.S. Department of Defense for support in the form of a graduate fellowship. We especially thank Yuan Lu and Steve Shepard for their technical assistance.

References

1. T. K. Wu, *Frequency Selective Surface and Grid Array* (Wiley, New York, 1995).
2. P. A. Krug, D. H. Dawes, R. C. McPhedran, W. Wright, J. C. Macfarlane, and L. B. Whitbourn, "Annular-slot arrays as far-infrared bandpass filters," Opt. Lett. **14,** 931–933 (1989).
3. C. M. Rhoades, E. K. Damon, and B. A. Munk, "Mid-infrared filters using conducting elements," Appl. Opt. **21,** 2814–2816 (1982).
4. I. Puscasu, D. Spencer, and G. D. Boreman, "Refractive-index and element-spacing effects on the spectral behavior of infrared frequency-selective surfaces," Appl. Opt. **39,** 1570–1574 (2000).
5. M. D. Morgan, W. E. Horne, V. Sundaram, J. C. Wolfe, S. V. Pendharkar, and R. Tiberio, "Application of optical filters fabricated by masked ion beam lithography," J. Vac. Sci. Technol. B **14,** 3903–3906 (1996).
6. K. J. Kogler and R. G. Pastor, "Infrared filters fabricated from submicron loop antenna arrays," Appl. Opt. **27,** 18–19 (1988).
7. Y. Xia and G. M. Whitesides, "Soft lithography," Angew. Chem. Int. Ed. Engl. **37,** 550–575 (1998).
8. Y. Xia, J. A. Rogers, K. E. Paul, and G. M. Whitesides, "Unconventional methods for fabricating and patterning nanostructures," Chem. Rev. **99,** 1823–1848 (1999).
9. J. A. Rogers, K. E. Paul, R. J. Jackman, and G. M. Whitesides, "Using an elastomeric phase mask for sub-100 nm photolithography in the optical near field," Appl. Phys. Lett. **70,** 2658–2660 (1997).

10. J. A. Rogers, K. E. Paul, R. J. Jackman, and G. M. Whitesides, "Generating ~90 nanometer features using near-field contact-mode photolithography with an elastomeric phase mask," J. Vac. Sci. Technol. B **26,** 59–68 (1998).
11. K. E. Paul, T. L. Breen, J. Aizenberg, and G. M. Whitesides, "Maskless lithography: embossed photoresist as its own optical element," Appl. Phys. Lett. **73,** 2893–2895 (1998).
12. J. Aizenberg, A. J. Black, and G. M. Whitesides, "Controlling local disorder in self-assembled monolayers by patterning the topology of their metallic supports," Nature (London) **394,** 868–871 (1998).
13. A. J. Black, K. E. Paul, J. Aizenberg, and G. M. Whitesides, "Patterning disorder in monolayer resists for the fabrication of sub-100-nm structures in silver, gold, silicon, and aluminum," J. Am. Chem. Soc. **121,** 8356–8365 (1999).
14. J. C. Love, K. E. Paul, and G. M. Whitesides, "Fabrication of nanometer-scale features by controlled isotropic wet chemical etching," Adv. Mater. **13,** 604–607 (2001).
15. J. Aizenberg, J. A. Rogers, K. E. Paul, and G. M. Whitesides, "Imaging the irradiance distribution in the optical near field," Appl. Phys. Lett. **71,** 3773–3775 (1997).
16. J. Aizenberg, J. A. Rogers, K. E. Paul, and G. M. Whitesides, "Imaging profiles of light intensity in the near field: applications to phase-shift photolithography," Appl. Opt. **37,** 2145–2152 (1998).
17. H. Schmid and B. Michel, "Siloxane polymers for high-resolution, high-accuracy soft lithography," Macromolecules **33,** 3042–3049 (2000).
18. Y. Xia, D. Qin, and G. M. Whitesides, "Microcontact printing with a cylindrical rolling stamp: a practical step toward automatic manufacturing of patterns with submicrometer-sized features," Adv. Mater. **8,** 1015–1017 (1996).